JOURNAL OF VIROLOGY, Nov. 2010, p. 10965–10973 Vol. 84, No. 21
0022-538X/10/$12.00 doi:10.1128/JVI.01335-10

Novel Nipah Virus Immune-Antagonism Strategy Revealed by Experimental and Computational Study▽†

Jeremy Seto,[1,2]‡ Liang Qiao,[1,2]‡ Carolin A. Guenzel,[3]§ Sa Xiao,[3]¶ Megan L. Shaw,[3] Fernand Hayot,[1,2] and Stuart C. Sealfon[1,2]*

Center for Translational Systems Biology[1] and Departments of Neurology[2] and Microbiology[3], Mount Sinai School of Medicine, New York, New York 10029

Received 23 June 2010/Accepted 7 August 2010

Nipah virus is an emerging pathogen that causes severe disease in humans. It expresses several antagonist proteins that subvert the immune response and that may contribute to its pathogenicity. Studies of its biology are difficult due to its high pathogenicity and requirement for biosafety level 4 containment. We integrated experimental and computational methods to elucidate the effects of Nipah virus immune antagonists. Individual Nipah virus immune antagonists (phosphoprotein and V and W proteins) were expressed from recombinant Newcastle disease viruses, and the responses of infected human monocyte-derived dendritic cells were determined. We developed an ordinary differential equation model of the infectious process that that produced results with a high degree of correlation with these experimental results. In order to simulate the effects of wild-type virus, the model was extended to incorporate published experimental data on the time trajectories of immune-antagonist production. These data showed that the RNA-editing mechanism utilized by the wild-type Nipah virus to produce immune antagonists leads to a delay in the production of the most effective immune antagonists, V and W. Model simulations indicated that this delay caused a disconnection between attenuation of the antiviral response and suppression of inflammation. While the antiviral cytokines were efficiently suppressed at early time points, some early inflammatory cytokine production occurred, which would be expected to increase vascular permeability and promote virus spread and pathogenesis. These results suggest that Nipah virus has evolved a unique immune-antagonist strategy that benefits from controlled expression of multiple antagonist proteins with various potencies.

Paramyxoviruses, which include Sendai virus, Newcastle disease virus (NDV), respiratory syncytial virus, measles virus, and mumps virus, cause disease in many species (10, 29, 46, 55, 65). Nipah virus (NiV) is a highly pathogenic zoonotic paramyxovirus and emerging pathogen of this family. NiV is in the genus *Henipavirus*, whose members are a source of public health and agricultural concern due to their ability to spread between species and to transmit through highly mobile reservoir species, specifically, the fruit-eating bats of the genus *Pteropus* (15, 19, 45, 63). NiV is thought to be transmitted via a respiratory route; it presents as acute febrile encephalitis, causes high mortality, and can manifest a dangerous secondary spread to contacts (8, 15, 19, 35). Like all viruses that are pathogenic for humans, NiV has evolved immune-antagonist proteins that suppress the human innate immune response and facilitate virus replication.

Innate immunity is triggered through a variety of pathogen recognition receptors, including Toll-like receptors (TLRs), NOD-like receptors, and RIG-I-like receptors. Antiviral genes are produced in response to nucleic acid detection by RIG-I or TLR3/7/8/9, resulting in signaling cascades that ultimately produce antiviral cytokines, particularly type I interferons (IFNs) (28, 36, 64). Virus interactions with their hosts have resulted in viral mechanisms to suppress their detection and host production of antiviral cytokines. One well-characterized example of such a viral immune antagonist is influenza virus nonstructural protein 1 (NS1), which interferes with IFN production to enhance pathogenicity (20, 22). Innate responses may be further dampened by viral suppression of cytokine signaling to prevent relay of the warning signals to uninfected cells. Combinatorial effects of immune inhibitors may increase the virulence and pathogenicity of invading viruses.

Paramyxoviruses produce a polymerase-associated phosphoprotein (P) that is necessary for viral replication. Through an idiosyncratic editing property of the viral polymerase, nontemplated guanine residues are inserted into the P-gene mRNA, resulting in genomic diversification from these frameshift mutations (7, 17, 26, 30, 37, 39, 43). These additional gene products have been demonstrated to interfere with IFN signaling (48, 59, 60). Editing in NiV produces a V protein and a W protein from the P gene (3, 12, 24, 50, 57). NiV V and W proteins have been shown to interact with signal transducer and activator of transcription 1 (STAT1) through the N-terminal domain shared with P, sequestering STATs in high-molecular-weight complexes (16, 54, 55). While NiV W and V proteins share identical N termini, the unique C terminus of NiV

* Corresponding author. Mailing address: Department of Neurology, Mount Sinai School of Medicine, 1 Gustave Levy Place, Box 1137, Annenberg Building 14-94B, Box 1137, New York, NY 10029. Phone: (212) 241-7076. Fax: (212) 860-4952. E-mail: stuart.sealfon@mssm.edu.

† Supplemental material for this article may be found at http://jvi.asm.org/.

‡ These authors contributed equally to the study.

§ Present address: Institut Cochin, Université Paris-Descartes, CNRS, UMR 8104, Paris, France.

¶ Present address: Virginia-Maryland Regional College of Veterinary Medicine, University of Maryland, College Park, MD 20742.

▽ Published ahead of print on 25 August 2010.

W contains a nuclear localization signal that compartmentalizes the effects of its interferon antagonism (56).

Much of the knowledge regarding the mechanisms of these immune suppressors has been obtained in epithelial transfection systems. While many studies have focused on molecular interactions of NiV immune antagonists, the underlying suppression of innate immunity is incompletely understood. The presentation of NiV infection as encephalitis with antigen-positive inclusions in the brain suggests that the systemic innate and adaptive responses opposing viral spread are suppressed (14). Dendritic cells (DCs) reside in tissue and represent a link between innate and adaptive immunity. Due to the presumed respiratory transmission of NiV, resident DCs encountering infected cells in the lungs may become infected and rendered inefficient at negating viral spread. The role of DCs as a target of NiV is unknown.

Research on NiV is difficult due to the highly pathogenic properties that have limited studies on the full virus to biosafety level 4 facilities (32, 34, 40, 47). The paramyxovirus NDV has been established as a useful vector with which to study the effects of immune antagonists from human viruses (20, 49). Because NDV has not adapted for infection of humans, it generates a strong immune response in human cells. Therefore, expression of immune antagonists from viruses pathogenic for humans as NDV recombinants allows measurement of the specific effects of the various antagonists in the context of a strong immune activator. However, the effects of an individual immune antagonist on host cell responses does not, by itself, reveal the overall multiantagonist strategy utilized by NiV. In order to make inferences about the immune-antagonist mechanisms of wild-type NiV from the studies with NDV recombinants expressing individual NiV proteins, we have used computational modeling to integrate data obtained with these viruses with published data on wild-type NiV. Our results suggest that NiV has evolved a novel strategy of regulated immune antagonism particularly suited for its overall life cycle and pathogenesis.

MATERIALS AND METHODS

Viruses and cells. Recombinant NDV(-V)/NDV-V has been described previously [(−V) indicates that endogenous V has been removed, and NDV-V indicates that it has been reinserted] (49). The P, V, and W genes of Nipah virus were inserted into an XbaI site between the P and M genes of the NDV(-V) cDNA clone. Each gene was amplified by PCR with restriction enzyme site-tagged primers: P forward (5′-CG**G CTA GC**T TAG AAA AAA ***T***AC GGG TAG AA*C ACT AGT CCG CCA CC*a tgg ata aat tgg aac tag tca ac), P reverse (5′-CGG CTA GCT CAA ATA TTA CCG TCA ATG ATG TC), V and W forward (5′-GC**T CTA GA**T TAG AAA AAA ***T***AC GGG TAG AA*T AGT CCG CCA CC*a tgg ata aat tgg aac tag tca ac), V reverse (5′-GC**T CTA GA**T TAA CCG CAG TGG AAG CAT TC), and W reverse (5′-GC**T CTA GA**C TAG TTG GAC ATT CTC CGC ATT G). XbaI and NheI are in boldface; the NDV gene start and gene end are underlined; the P, V, and W genes are in lowercase; and one intergenic nucleotide T is shown in boldface italics. The plasmids pCAGGS-NiV-P, -V, and -W containing mutations to remove the C open reading frame (ORF) were used as templates for PCR amplification (49, 57). The PCR products and NDV(-V) vector were digested with XbaI or NheI. After purification by a PCR purification kit (Qiagen), the fragments and vector were ligated by a rapid ligation kit (Roche). All constructs were confirmed by sequencing. The rescue of recombinant NDV-NiV-P, NDV-NiV-V, and NDV-NiV-W viruses followed the procedures described previously (42, 49).

All recombinant NDVs were grown in 10-day-old embryonated chicken eggs. Viruses were titrated on DF1 cells by plaque assay (25) and detected via immunostaining with an antinucleoprotein polyclonal antibody (Mount Sinai Hybridoma Facility). Virus infections of DF1 cells were performed in infection medium (Dulbecco's modified Eagle medium, 1% bovine serum albumin, 0.15% $NaHCO_3$, 10% allantoic fluid from 10-day-old embryonated chicken eggs). Virus infections in Vero cells were performed in infection medium (Dulbecco's modified Eagle medium, 1% bovine serum albumin, 1% penicillin-streptomycin, 10% allantoic fluid from 10-day-old embryonated chicken eggs).

Isolation and culture of human DCs. Peripheral blood mononuclear cells were isolated by Ficoll density gradient centrifugation (Histopaque; Sigma Aldrich) from buffy coats of healthy human donors (New York Blood Center). $CD14^+$ cells were magnetically purified using anti-human CD14 magnetic beads on Midimacs LS columns (Miltenyi Biotec). After elution from the columns, $CD14^+$ cells were plated (1×10^6 cells/ml) in DC medium (RPMI, 10% fetal bovine serum, 100 units/ml of penicillin, 100 μg/ml streptomycin) supplemented with 500 U/ml human granulocyte-macrophage colony-stimulating factor (Peprotech) and 1,000 U/ml human interleukin-4 (IL-4; Peprotech) and incubated for 5 days at 37°C. DCs (1×10^6 cells/ml) were infected at a multiplicity of infection (MOI) of 0.5 for 2, 4, 8, 12, and 16 h postinfection.

Western blot analysis. Infected dendritic cells were harvested at 8 h, washed in phosphate-buffered saline (PBS), and lysed in RIPA buffer (150 mM NaCl, 20 mM Tris, 2 mM EDTA, 1% NP-40, 0.25% deoxycholate, 1 mM NaF, and 1 mM Na_3VO_4 supplemented with complete mini-EDTA-free protease inhibitors [Roche]). Protein was quantified by a Bio-Rad protein assay, and 30 μg was resuspended in Laemmli buffer. Samples were denatured for 10 min at 100°C and resolved by SDS-PAGE. Gels were transferred to nitrocellulose and immunoblotted with a polyclonal rabbit anti-NDV raised against the NDV La Sota strain (gift of Peter Palese) and mouse anti-glyceraldehyde-3-phosphate dehydrogenase (GAPDH; Santa Cruz Biotechnology). Blots were stained with goat anti-rabbit IRDye 680 and goat anti-mouse IRDye 800CW (Li-Cor) and scanned on an Odyssey infrared imaging system (Li-Cor). The fluorescence of specific bands was quantified with Odyssey software (Li-Cor).

Flow cytometry. Cells were fixed with 1.5% paraformaldehyde (Electron Microscopy Sciences) after 12 h of infection and washed in PBS supplemented with 2% bovine serum albumin (Sigma-Aldrich). Infected cells were stained with a monoclonal antibody for HLA-ABC (BD Pharmingen) and assayed on an LSRII flow cytometer (Beckman Coulter). Analysis of flow cytometry data was performed with FlowJo software (Tree Star).

Capture ELISAs. Capture enzyme-linked immunosorbent assays (ELISAs) for alpha 2 IFN (IFN-α2), tumor necrosis factor alpha (TNF-α), IL-6, IL-8, monocyte chemoattractant protein 1 (MCP-1), chemokine ligand 4 (CCL4), IP10, and CCL5 (Millipore) were performed, following the manufacturer's protocol, as part of a multiplex assay. Plates were read in a Luminex plate reader, and data were analyzed using software from Applied Cytometry Systems. All samples were assayed in duplicate or triplicate. IFN-β ELISAs (PBL Interferon Source) were performed separately.

Quantitative real-time PCR. RNA from infected DCs was isolated and treated with DNase by using an Absolutely RNA reverse transcription-PCR (RT-PCR) microprep kit (Stratagene). Quantitative RT-PCR of the extracted RNAs was performed by using a previously published SYBR green protocol with an ABI 7900 HT thermal cycler by the Mount Sinai Quantitative PCR Shared Research Facility. Each transcript in each sample was assayed in triplicate, and the median cycle threshold was used to calculate the copy number on the basis of the methodology established by (66) using three housekeeping genes (actin, rps11, and tubulin) for normalization.

Model description and parameter estimation. The present model is an extension of our previous model of viral infection of DCs pretreated with IFN-β (52). It includes the same species and parameters and incorporates the same network of reactions, comprising the IFN-β positive-feedback loop and the negative-feedback loop associated with suppressors of cytokine signaling (SOCS) in the Jak/STAT pathway. It is extended through the introduction of the positive-feedback loop attached to TNF-α and the induction of chemokines CCL4 and CCL5. For simplicity, various model assumptions were made. A more complete description of the model assumptions is found in the supplemental material. For example, STAT1 and STAT2 were not differentiated and were modeled as one species, denoted STAT. Moreover, in order to avoid the introduction of reactions involving unmeasured quantities, such as the time courses of IFN-β transcription factors and the concomitant increase in the number of unknown reaction parameters, we represented the whole viral sensing network by two paths connected to the viral sensor. The first one is responsible for the induction of TNF-α, CCL4, and STAT and participates with the second one in the induction of IFN-β and CCL5. The second one corresponds to interferon regulatory factor 7 (IRF7), which is singled out because its induction after Jak/STAT pathway activation plays a major role in IFN-β production (4) (see Fig. 5).

Simplifications of the model signaling network are required due to our ignorance of the interplay between viral sensing and immune antagonism by NiV P

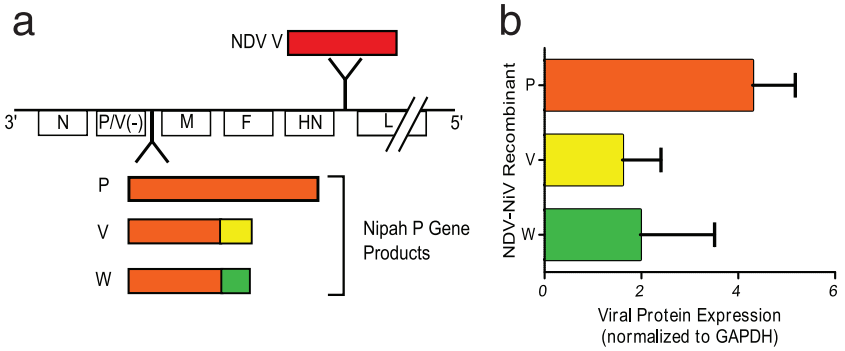

FIG. 1. (a) Schematic representation of recombinant NDVs expressing NDV V, NiV P, NiV V, or NiV W protein. NDV(-V) served as a backbone for these viruses. NiV ORFs were inserted between the P and M genes, while NDV V was inserted between the HN and L genes and is subsequently referred to as NDV. (b) There are no significant differences in the levels of viral proteins expressed in dendritic cells infected with recombinant NDV expressing P, V, or W at 8 h ($P = 0.26$, analysis of variance).

and edited variants. We know that W protein exercises its antagonistic effects in the nucleus, whereas P and V protein do so in the cytoplasm. As to their action in the Jak/STAT pathway, we know that all three proteins prevent STAT phosphorylation and, consequently, the induction of interferon-responsive genes, such as IRF7 and antiviral genes. Inhibition of IRF7 in turn affects induction of IFN-α/β (Fig. 5). We therefore assume that P, V, and W interfere in the signaling network at different levels of the first pathway described above and do so in an independent manner. The path associated with IRF7 is not affected in this way (see Fig. 5). IRF7 is, however, interfered with by the actions of P, V, and W in the Jak/STAT pathway, where all three tend to sequester STAT in order to disrupt signaling, which requires STAT phosphorylation through the activated tyrosine kinase 2 (Tyk2)/Jak complex after ligand binding to the IFN-α/β receptor (IFNAR) (see Fig. 5). In the Jak/STAT pathway, P, V, and W act additively, since they compete for the available STAT. Our model contains 14 species and a total of 49 parameters. The parameter values were estimated through an iterative nonlinear least-squares fitting to the experimental data. The starting parameter values of mRNA induction, degradation, and protein translation rate constants were set equal to the corresponding typical values (see the table in the supplemental material). For the remaining parameters, we set their starting values equal to physiologically reasonable numbers. The initial condition of our model corresponds to a state in which STAT is set equal to 0.1 μM and the concentrations of the remaining modeled species are set equal to zero. The fitting procedure relied on an error function which was used as well to study parameter sensitivity. For the group of optimized parameters, we calculated confidence levels and determined their identifiability. For the simulation of the wild-type NiV infection in DCs, we use the V, P, and W editing frequencies reported in 293T cells (32) to parameterize the temporal kinetics of expression of these proteins in the DCs. Details of the parameter-fitting process can be found in the supplemental material.

RESULTS

Suppression of maturation in human dendritic cells. All four NiV P-gene products have previously been demonstrated to act as IFN antagonists in epithelial cell lines, where they suppress the antiviral response (16, 50, 53, 54, 56, 57). We generated recombinant Newcastle disease viruses each expressing a different NiV immune antagonist to study the effects in the context of a strong immune activator (Fig. 1a). Western blot analysis (Fig. 1b) of DCs infected with recombinant NDV revealed that viral protein expression was comparable among viruses expressing NiV immune antagonists. As sentinel immune cells resident at tissue/environmental barriers, DCs represent a link between viral infection and activation of innate to adaptive responses to neutralize diverse pathogens. Infected DCs process virus particles and display them to adaptive immune cells through major histocompatibility complex class I (MHC-I). Direct infection of human monocyte-derived DCs with NDV results in increased surface expression of the MHC-I marker HLA-ABC. Infection by NDV chimeras expressing NiV immune-antagonist proteins blocks this upregulation and results in baseline levels of HLA-ABC (Fig. 2). Such a blockade of MHC-I *in vivo* would likely interfere with the review of antigens by T cells and facilitate the spread of infection.

Following infection of cultured DCs by NDV, a large increase in the amount of type I IFN mRNA is observed within 8 h (Fig. 3). However, infection by recombinant NDVs expressing NiV proteins markedly attenuates this response. In addition to inhibition of IFN, NiV chimeras also suppress the production of mRNA encoding inflammatory chemokines,

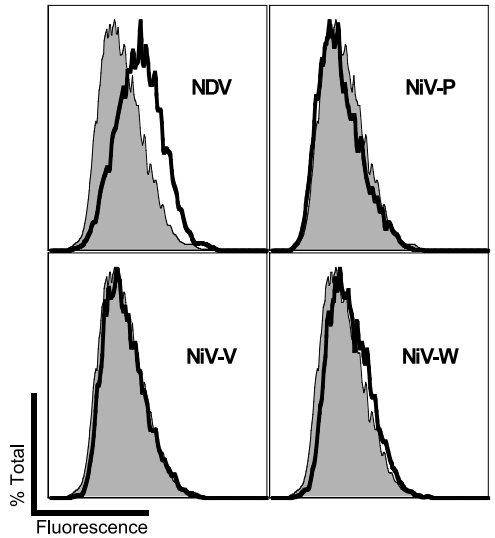

FIG. 2. Nipah virus immune antagonists suppress upregulation of surface MHC-I in human dendritic cells. Cells were infected with NDV or recombinant NDV expressing NiV proteins P, V, and W; and the surface levels of MHC-I were determined by flow cytometry. Infection with NDVs expressing NiV antagonists (heavy solid lines) returned the level of surface expression of MHC-I to that of the baseline (shaded). The results obtained with NiV P, V, and W in multiple experiments were not significantly different from each other (data not shown).

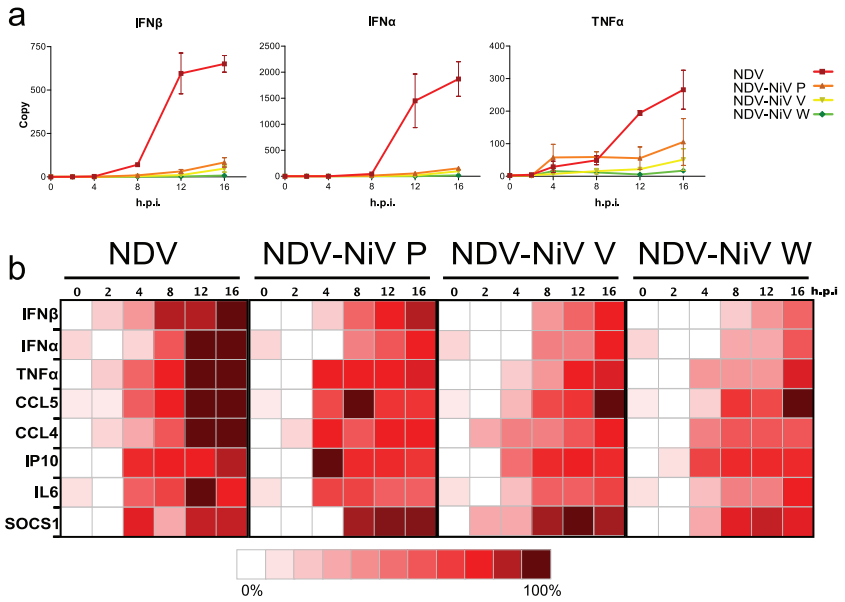

FIG. 3. Gene expression profiles from recombinant NDV-NiV infection. Cells infected with these viruses demonstrated suppressed activation profiles compared to the NDV profile. (a) NiV protein-expressing viruses show strong inhibition of IFN-α/β as well as the inflammatory cytokine TNF-α (h.p.i., hours postinfection). (b) Summary PCR data in heat maps demonstrate the average responses of gene induction changes over time being suppressed/delayed by NiV proteins P, V, and W. Data are normalized to maximum induction of each gene after $\log_2$ transformation.

such as TNF-α, CCL4, and CCL5, and of IFN-induced genes, such as MxA and ISG54 (data not shown). For all responses tested, the NiV W protein showed the strongest inhibitory effects, followed by NiV V. While strongly inhibiting virus-induced gene induction, NiV P was not as potent as V and W in suppressing immune responses. Concordant with the diminished transcriptional response to virus infection, multiplex ELISA revealed an attenuated secretion of virus-induced cytokines (Fig. 4). The concordance of the protein and mRNA measurements appears to be greater for TNF-α and CCL5 than for IFN-β (Fig. 3 and 4). These differences may arise from differences in the assay methodology utilized for IFN and the

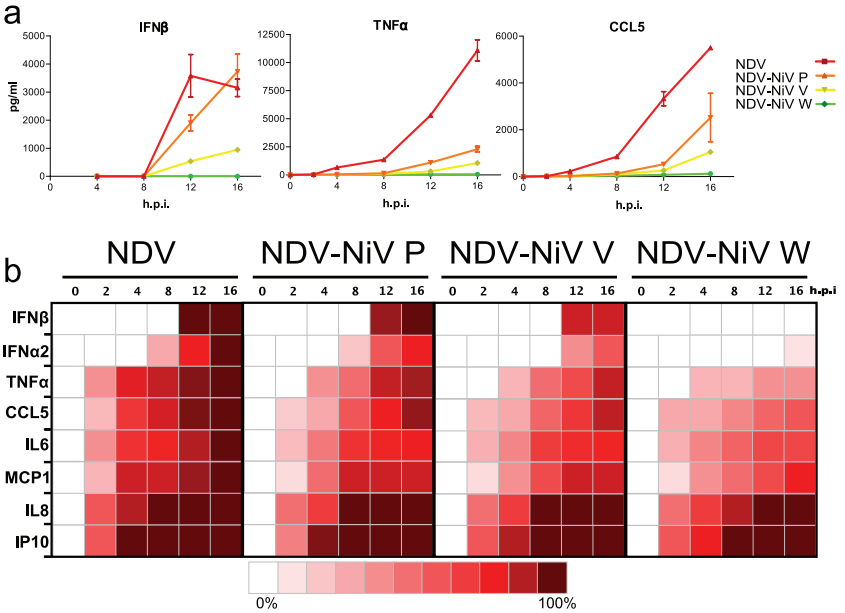

FIG. 4. ELISA and multiplex ELISAs of cytokines from virus-infected cells. Infection of human DCs by NDV provoked strong responses in cytokine production. (a) Interferon was produced in abundance upon infection with NDV, while NiV proteins P, V, and W delayed production and release or completely abolished production (NiV W). Inflammatory cytokines TNF-α and CCL5 were similarly reduced in NDV-NiV infections. h.p.i., hours postinfection. (b) Summary multiplex ELISA data as heat maps normalized to the maximum amount of protein secreted for each cytokine after $\log_2$ transformation. Assays for all cytokines except IFN-β were performed simultaneously using multiplex ELISA. IFN-β was measured using conventional ELISA.

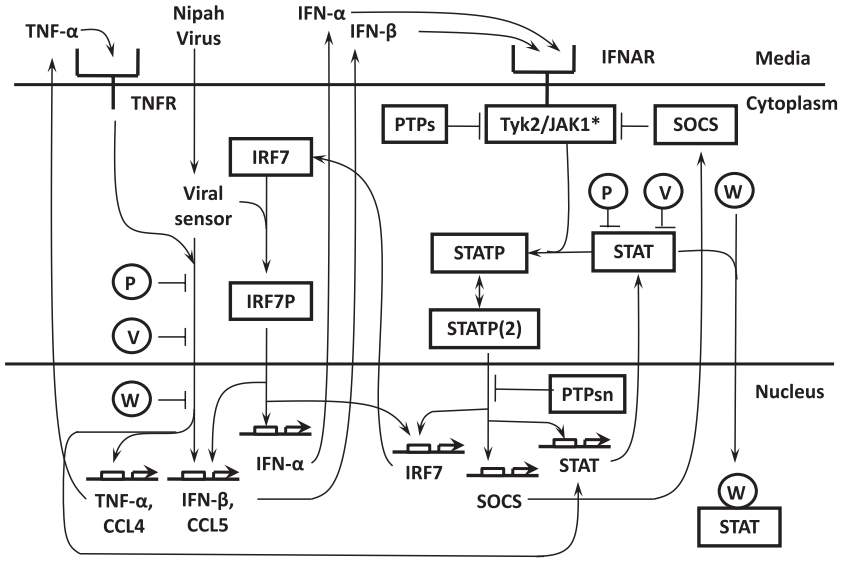

FIG. 5. Model schematic of Nipah virus-triggered DC immune response mechanisms and antagonist activity of the response. Detection of Nipah virus by viral sensors leads to the induction of the genes for IFNs and TNF-α, together with other genes, such as those for CCL4 and CCL5, through two positive-feedback loops mediated through the Jak/STAT pathway and NFκB, respectively. Nipah virus encodes antagonist proteins P, V, and W, which can effectively suppress the DC immune responses by targeting the key mediators in both the induction feedback loops.

other cytokines as well as differences in the regulatory mechanisms controlling IFN expression at the RNA and protein levels.

Mathematical model of NiV infection of DCs. In order to explore the effects of NiV immune antagonists on DCs during infection, we created a mathematical model of the responses of DCs to NiV infection that incorporates our experimental data, as well as results for the wild-type NiV available in the literature (Fig. 5) (32, 34). The model reaction network comprises 14 ordinary differential equations (ODEs). The hypotheses underlying the development of the model and the equations used for simulation are presented in Materials and Methods and in the supplemental material. The model consists of a generic virus-sensing mechanism that stimulates interferon production and interferon signaling that induces other antiviral response genes. All the NiV antagonists interfere with both viral sensing and specific components of cytokine STAT signaling, as reported in the experimental literature (3, 12, 53, 56, 57). Our data support the modeling assumption that P interferes with viral sensing.

The model, which has a minimal number of free parameters, aims to capture the essential characteristics of the experimental time course data for seven of the species that are measured experimentally: mRNA of IFN-β (IFN-β_m), mRNA of IFN-α (IFN-α_m), mRNA of TNF-α (TNF-α_m), IFN-α secreted into the extracellular environment (IFN-α_{env}), TNF-α secreted into the extracellular environment (TNF-α_{env}), mRNA of CCL4 ($CCL4_m$), and mRNA of CCL5 ($CCL5_m$). These cytokines and chemokines signal the state of activation of the DCs and serve as markers of the strength of the antiviral response and the effects of viral antagonism. The amount of IFN-$\alpha_{m,}$ which depends on activated IRF7, itself induced in the Jak/STAT pathway, reflects the strength of that pathway (as does the amount of IFN-β at times after viral infection), whereas the induction of TNF-α, CCL4, and CCL5 (as well as that of IFN-β) is influenced by activation of the complex signaling network attached to viral sensors (Fig. 5). The model consists of three spatial compartments: cytoplasm, nucleus, and extracellular space with membrane receptors for IFN-α/β and TNF-α. Contributions from other dendritic cells to extracellular amounts of IFN-α/β_{env} and TNF-α_{env} are taken into account in the equations by the factor *C* (see equations S29 to S42 in the supplemental material), which denotes the concentration of virus-infected dendritic cells.

We initially simulated the effects of infection with the NDV chimeras that we studied experimentally. The results of simulation are shown by continuous lines in Fig. 6, with the actual experimental measurements indicated in the same figure by symbol markers. The correspondence of the model simulations and the experimental measurement is high; thus, the model recapitulates the main qualitative impression of the experimental results. Namely, P causes a modest suppression of the immune response induced by NDV infection. In contrast, V causes a much greater suppression, and W leads to an essentially complete elimination of the antiviral response in DCs.

The recombinant virus experiments are limited to determination of the effects of single antagonists. During infection, wild-type NiV generates each of these proteins according to different time courses. The experimental data alone do not illuminate why NiV has evolved this complex pattern of immune-antagonist production. The goal of the modeling was to use the available data and the results of the present study to re-create the profile of responses that occur during infection by a wild-type virus and thereby to elucidate the overall immune-antagonist strategy used by NiV. Therefore, in order to gain insight into the immune response during actual NiV infection, we proceeded to simulate the effects of all three immune antagonists expressed in a temporal pattern derived from published experiments with wild-type virus (32, 34). The experimental data on viral antagonist expression was obtained with

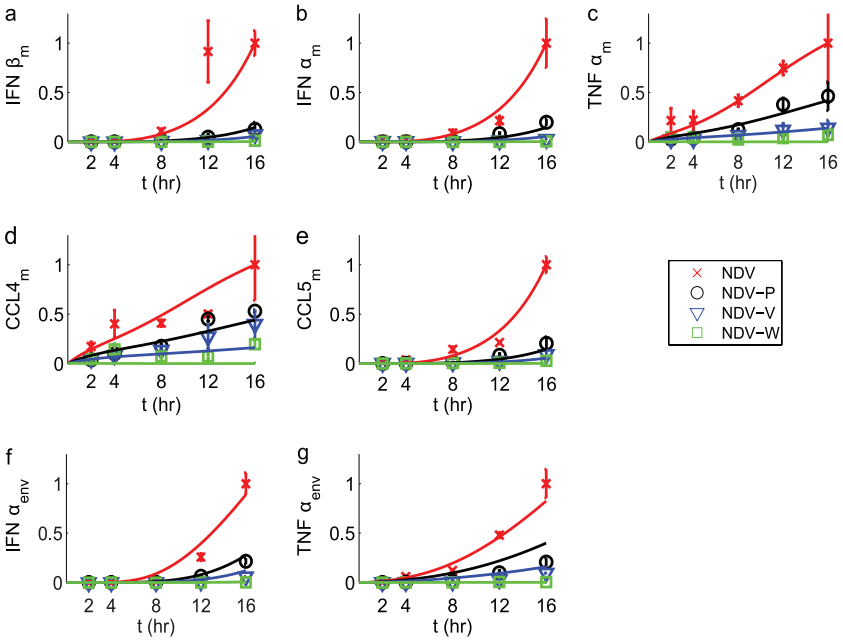

FIG. 6. Superimposition of model simulations (solid lines) and experimental measurements (symbols) of DC responses to NDV and Nipah chimera virus infection. The experimental time course data points are normalized to the maximal response and are marked by crosses, circles, triangles, and squares for the NDV control and chimera viruses encoding the NiV proteins P, V, and W, respectively. Each data point represents the average of three experimental replicates. The simulation result is plotted with solid lines and normalized to the corresponding maximum. The label of the horizontal axis represents the time (in hours) after viral infection (time zero). (a) IFN-β mRNA; (b) IFN-α mRNA; (c) TNF-α mRNA; (d) CCL4 mRNA; (e) CCL5 mRNA; (f) IFN-α in the medium; (g) TNF-α in the medium.

293T cells. For the modeling, we assume that these results are relevant to human DCs.

To account for the additional time necessary for protein translation, simulations for wild-type NiV were delayed by 1 h. Relative levels of expression of NiV P, V, and W over time are shown in Fig. 7a. The demonstration that the measurements from the model simulations of the NDV recombinants closely resemble the experimental measurements of regulated genes (Fig. 6) provides some confidence in the accuracy of the simulations of gene induction with wild-type NiV infection in human DCs. The NDV-NiV W chimera causes almost complete suppression of gene responses (Fig. 3 and 6). Notably, the simulation of wild-type NiV infection in DCs shows a much greater induction of TNF-α and CCL4 mRNAs at early time points (Fig. 7b and c). In contrast, the induction of IFN was effectively suppressed by the wild-type virus at early time points (data not shown). Later in the infection, the simulation shows that the wild-type NiV completely shuts down both inflammatory and antiviral cytokine production.

DISCUSSION

We show that the various immune antagonists produced by NiV have different effects on the immune response of human dendritic cells. All three immune antagonists suppress antiviral cytokines, but the W protein, in particular, is much more efficient at suppressing inflammatory cytokine production. In addition to the sequential suppression of cytokine production in response to NiV antagonist-expressing viruses, we observed the inhibition of other innate immune responses that may facilitate the pathogenicity of NiV in a manner consistent with the role that dendritic cells play in innate to adaptive immunity transitions. As antigen-presenting cells, directing the adaptive immune response is necessary for effective pathogen clearance from the body. However, the suppression of MHC-I upregulation suggests a potent deficiency in initiating the adaptive response. Suppression of antigen presentation by MHC-I is employed by multiple virus types to evade immune clearance, thereby promoting persistent infections (1, 2, 5, 6, 18, 51, 61). The identification of viral antigen in the brains of NiV encephalitis patients postmortem indicates the spread of the virus past the presumed respiratory route of entry (13, 27). DCs have also been known to provide privileged havens for viruses and have been indicated in the systemic spread of Ebola virus and Dengue virus (9, 21, 33, 38, 44). Additionally, relapse and late-onset encephalitis from Nipah virus infections suggest viral persistence associated with long-term immune evasion (58).

We developed a mathematical model of the major reaction networks involved in NDV-induced immune activation that reproduced gene expression profiles activated by NDV and NDV chimeras expressing NiV antagonists. One simplifying assumption of the model is that it does not include interaction effects among viral proteins. It is known that the nucleocapsid protein (N) interacts with the carboxyl terminus of NiV P as a part of the polymerase complex (11, 23). While we are unaware of evidence for interactions between NiV N and V or W, it is possible that these occur. Our experimental system does not allow the assessment of the interaction of P/V/W with other NiV proteins, and the

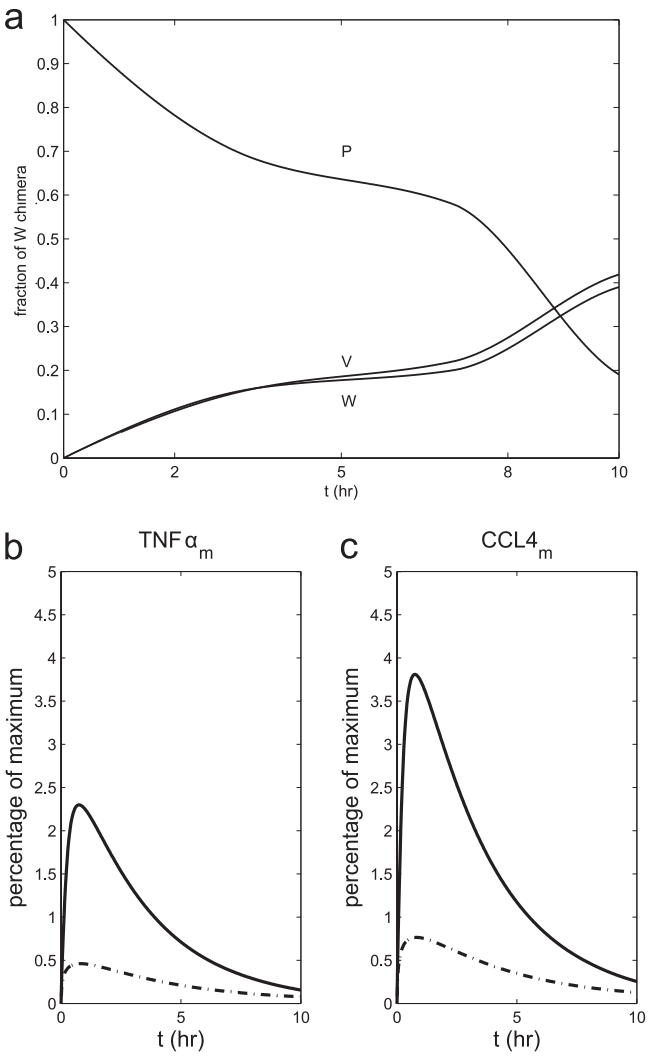

FIG. 7. (a) Proportional representation of Nipah virus P, V, and W over time from wild-type NiV extrapolated from previously published data regarding the editing frequencies (32) used to parameterize the concentration of each protein. (b and c) Predicted immune response for wild-type Nipah virus compared to that induced by NDV recombinant viruses expressing individual Nipah virus immune-antagonist proteins. Simulation of TNF-α mRNA (b) and CCL4 mRNA (c) by wild-type NiV (solid lines) is compared with that by the NDV-NiV W chimera (broken lines). Measurements are noted as a percentage of the maximal response of the NDV-NiV P chimera. Note that the NDV expressing W causes more efficient suppression of the inflammatory than either wild-type Nipah virus. t, time.

model does not include these types of interactions. By fitting the model with previously published profiles of NiV protein expression in wild-type infections, we predict a partial suppression of immune activation elicited at early time points of wild-type NiV infection. NiV P is the dominantly expressed protein during early times of infection. Over time, a greater proportion of the nongenomically encoded NiV V and W proteins are produced. The results of the model simulations show a high degree of correlation with experimental data and indicate that wild-type Nipah virus allows some dendritic cells to produce inflammatory cytokines.

The finding that wild-type Nipah virus is less efficient than a recombinant NDV expressing only the W protein at suppressing all aspects of the immune response in infected human cells is surprising. Our expectation was that the wild-type virus would combine the expression of the various immune antagonists to lead to maximal suppression of the cell response. However, the method of production of these immune antagonists by the wild-type virus does not lead to this result. In the NDV-NiV W recombinant, the protein is directly encoded and efficiently produced by transcription at the beginning of infection. In the wild-type virus, the antagonists are generated by RNA editing, and this leads to a delay in the production of high levels of W (32). Although the simulation attempts to recapitulate the effects of wild-type Nipah virus infection in human DCs *in vitro*, it is interesting to consider the implications of these simulations on NiV infection *in vivo*. We speculate that the lack of immune antagonism at early times may contribute to NiV pathogenesis by increasing vascular permeability and virus dissemination (31, 41, 62).

The present study demonstrates the importance of integrating experimental data and mathematical simulations to explore the biology of highly pathogenic viruses. Modeling allows all available experimental data to be utilized to provide insight into aspects of the behavior of the wild-type virus that may be difficult or impossible to measure experimentally. Models may also be valuable for testing and refining therapeutic approaches to infections with pathogenic viruses.

ACKNOWLEDGMENT

This work was supported by contract HHSN266200500021C from the National Institute of Allergy and Infectious Diseases.

REFERENCES

1. **Abendroth, A., I. Lin, B. Slobedman, H. Ploegh, and A. M. Arvin.** 2001. Varicella-zoster virus retains major histocompatibility complex class I proteins in the Golgi compartment of infected cells. J. Virol. **75:**4878–4888.
2. **Ali, A., H. L. Ng, M. D. Dagarag, and O. O. Yang.** 2005. Evasion of cytotoxic T lymphocytes is a functional constraint maintaining HIV-1 Nef expression. Eur. J. Immunol. **35:**3221–3228.
3. **Andrejeva, J., K. S. Childs, D. F. Young, T. S. Carlos, N. Stock, S. Goodbourn, and R. E. Randall.** 2004. The V proteins of paramyxoviruses bind the IFN-inducible RNA helicase, mda-5, and inhibit its activation of the IFN-beta promoter. Proc. Natl. Acad. Sci. U. S. A. **101:**17264–17269.
4. **Apostolou, E., and D. Thanos.** 2008. Virus infection induces NF-kappa B-dependent interchromosomal associations mediating monoallelic IFN-beta gene expression. Cell **134:**85–96.
5. **Bartee, E., M. Mansouri, B. T. Hovey Nerenberg, K. Gouveia, and K. Fruh.** 2004. Downregulation of major histocompatibility complex class I by human ubiquitin ligases related to viral immune evasion proteins. J. Virol. **78:**1109–1120.
6. **Benz, C., and H. Hengel.** 2000. MHC class I-subversive gene functions of cytomegalovirus and their regulation by interferons—an intricate balance. Virus Genes **21:**39–47.
7. **Blum, L. S., R. Khan, N. Nahar, and R. F. Breiman.** 2009. In-depth assessment of an outbreak of Nipah encephalitis with person-to-person transmission in Bangladesh: implications for prevention and control strategies. Am. J. Trop. Med. Hyg. **80:**96–102.
8. **Bobbitt, K. R., M. M. Addo, M. Altfeld, T. Filzen, A. A. Onafuwa, B. D. Walker, and K. L. Collins.** 2003. Rev activity determines sensitivity of HIV-1-infected primary T cells to CTL killing. Immunity **18:**289–299.
9. **Bray, M., and T. W. Geisbert.** 2005. Ebola virus: the role of macrophages and dendritic cells in the pathogenesis of Ebola hemorrhagic fever. Int. J. Biochem. Cell Biol. **37:**1560–1566.
10. **Carrigan, D. R., and C. M. Kabacoff.** 1987. Identification of a nonproductive, cell-associated form of measles virus by its resistance to inhibition by recombinant human interferon. J. Virol. **61:**1919–1926.
11. **Chan, Y. P., C. L. Koh, S. K. Lam, and L. F. Wang.** 2004. Mapping of

domains responsible for nucleocapsid protein-phosphoprotein interaction of henipaviruses. J. Gen. Virol. **85:**1675–1684.
12. **Childs, K., N. Stock, C. Ross, J. Andrejeva, L. Hilton, M. Skinner, R. Randall, and S. Goodbourn.** 2007. mda-5, but not RIG-I, is a common target for paramyxovirus V proteins. Virology **359:**190–200.
13. **Chong, H. T., and C. T. Tan.** 2003. Relapsed and late-onset Nipah encephalitis, a report of three cases. Neurol. J. Southeast Asia **8:**109–112.
14. **Chua, K. B.** 1999. Fatal encephalitis due to Nipah virus among pig-farmers in Malaysia. Lancet **354:**1257–1259.
15. **Chua, K. B.** 2003. Nipah virus outbreak in Malaysia. J. Clin. Virol. **26:**265–275.
16. **Ciancanelli, M. J., V. A. Volchkova, M. L. Shaw, V. E. Volchkov, and C. F. Basler.** 2009. Nipah virus sequesters inactive STAT1 in the nucleus via a P gene-encoded mechanism. J. Virol. **83:**7828–7841.
17. **Curran, J., R. Boeck, and D. Kolakofsky.** 1991. The Sendai virus P gene expresses both an essential protein and an inhibitor of RNA synthesis by shuffling modules via mRNA editing. EMBO J. **10:**3079–3085.
18. **Dasgupta, A., E. Hammarlund, M. K. Slifka, and K. Fruh.** 2007. Cowpox virus evades CTL recognition and inhibits the intracellular transport of MHC class I molecules. J. Immunol. **178:**1654–1661.
19. **Enserink, M.** 2000. Emerging diseases. Malaysian researchers trace Nipah virus outbreak to bats. Science **289:**518–519.
20. **Fernandez-Sesma, A., S. Marukian, B. J. Ebersole, D. Kaminski, M. S. Park, T. Yuen, S. C. Sealfon, A. Garcia-Sastre, and T. M. Moran.** 2006. Influenza virus evades innate and adaptive immunity via the NS1 protein. J. Virol. **80:**6295–6304.
21. **Fuller, C. M., M. S. Collins, and D. J. Alexander.** 2009. Development of a real-time reverse-transcription PCR for the detection and simultaneous pathotyping of Newcastle disease virus isolates using a novel probe. Arch. Virol. **154:**929–937.
22. **Hale, B. G., R. E. Randall, J. Ortin, and D. Jackson.** 2008. The multifunctional NS1 protein of influenza A viruses. J. Gen. Virol. **89:**2359–2376.
23. **Halpin, K., B. Bankamp, B. H. Harcourt, W. J. Bellini, and P. A. Rota.** 2004. Nipah virus conforms to the rule of six in a minigenome replication assay. J. Gen. Virol. **85:**701–707.
24. **Harcourt, B. H., A. Tamin, T. G. Ksiazek, P. E. Rollin, L. J. Anderson, W. J. Bellini, and P. A. Rota.** 2000. Molecular characterization of Nipah virus, a newly emergent paramyxovirus. Virology **271:**334–349.
25. **Harper, D. R.** 1989. A novel plaque assay system for paramyxoviruses. J. Virol. Methods **25:**347–350.
26. **Hausmann, S., J. P. Jacques, and D. Kolakofsky.** 1996. Paramyxovirus RNA editing and the requirement for hexamer genome length. RNA **2:**1033–1045.
27. **Hegde, N. R., R. A. Tomazin, T. W. Wisner, C. Dunn, J. M. Boname, D. M. Lewinsohn, and D. C. Johnson.** 2002. Inhibition of HLA-DR assembly, transport, and loading by human cytomegalovirus glycoprotein US3: a novel mechanism for evading major histocompatibility complex class II antigen presentation. J. Virol. **76:**10929–10941.
28. **Heim, M. H.** 2005. RIG-I: an essential regulator of virus-induced interferon production. J. Hepatol. **42:**431–433.
29. **Homann, H. E., P. H. Hofschneider, and W. J. Neubert.** 1990. Sendai virus gene expression in lytically and persistently infected cells. Virology **177:**131–140.
30. **Jacques, J. P., S. Hausmann, and D. Kolakofsky.** 1994. Paramyxovirus mRNA editing leads to G deletions as well as insertions. EMBO J. **13:**5496–5503.
31. **Kim, S. S., C. Ye, P. Kumar, I. Chiu, S. Subramanya, H. Wu, P. Shankar, and N. Manjunath.** 2010. Targeted delivery of siRNA to macrophages for anti-inflammatory treatment. Mol. Ther. **18:**993–1001
32. **Kulkarni, S., V. Volchkova, C. F. Basler, P. Palese, V. E. Volchkov, and M. L. Shaw.** 2009. Nipah virus edits its P gene at high frequency to express the V and W proteins. J. Virol. **83:**3982–3987.
33. **Kyle, J. L., P. R. Beatty, and E. Harris.** 2007. Dengue virus infects macrophages and dendritic cells in a mouse model of infection. J. Infect. Dis. **195:**1808–1817.
34. **Lo, M. K., B. H. Harcourt, B. A. Mungall, A. Tamin, M. E. Peeples, W. J. Bellini, and P. A. Rota.** 2009. Determination of the henipavirus phosphoprotein gene mRNA editing frequencies and detection of the C, V and W proteins of Nipah virus in virus-infected cells. J. Gen. Virol. **90:**398–404.
35. **Mackenzie, J. S., H. E. Field, and K. J. Guyatt.** 2003. Managing emerging diseases borne by fruit bats (flying foxes), with particular reference to henipaviruses and Australian bat lyssavirus. J. Appl. Microbiol. **94**(Suppl.)**:**59S–69S.
36. **Malmgaard, L., J. Melchjorsen, A. G. Bowie, S. C. Mogensen, and S. R. Paludan.** 2004. Viral activation of macrophages through TLR-dependent and -independent pathways. J. Immunol. **173:**6890–6898.
37. **Malur, A. G., M. A. Hoffman, and A. K. Banerjee.** 2004. The human parainfluenza virus type 3 (HPIV 3) C protein inhibits viral transcription. Virus Res. **99:**199–204.
38. **Martinez, O., C. Valmas, and C. F. Basler.** 2007. Ebola virus-like particle-induced activation of NF-kappaB and Erk signaling in human dendritic cells requires the glycoprotein mucin domain. Virology **364:**342–354.
39. **Matsuoka, Y., J. Curran, T. Pelet, D. Kolakofsky, R. Ray, and R. W. Compans.** 1991. The P gene of human parainfluenza virus type 1 encodes P and C proteins but not a cysteine-rich V protein. J. Virol. **65:**3406–3410.
40. **Middleton, D. J., C. J. Morrissy, B. M. van der Heide, G. M. Russell, M. A. Braun, H. A. Westbury, K. Halpin, and P. W. Daniels.** 2007. Experimental Nipah virus infection in pteropid bats (Pteropus poliocephalus). J. Comp. Pathol. **136:**266–272.
41. **Muhl, H., and C. A. Dinarello.** 1997. Macrophage inflammatory protein-1 alpha production in lipopolysaccharide-stimulated human adherent blood mononuclear cells is inhibited by the nitric oxide synthase inhibitor N(G)-monomethyl-L-arginine. J. Immunol. **159:**5063–5069.
42. **Nakaya, T., J. Cros, M. S. Park, Y. Nakaya, H. Zheng, A. Sagrera, E. Villar, A. Garcia-Sastre, and P. Palese.** 2001. Recombinant Newcastle disease virus as a vaccine vector. J. Virol. **75:**11868–11873.
43. **Nayak, B., S. Kumar, P. L. Collins, and S. K. Samal.** 2008. Molecular characterization and complete genome sequence of avian paramyxovirus type 4 prototype strain duck/Hong Kong/D3/75. Virol. J. **5:**124.
44. **Nightingale, Z. D., C. Patkar, and A. L. Rothman.** 2008. Viral replication and paracrine effects result in distinct, functional responses of dendritic cells following infection with dengue 2 virus. J. Leukoc. Biol. **84:**1028–1038.
45. **Olson, J. G., C. Rupprecht, P. E. Rollin, U. S. An, M. Niezgoda, T. Clemins, J. Walston, and T. G. Ksiazek.** 2002. Antibodies to Nipah-like virus in bats (Pteropus lylei), Cambodia. Emerg. Infect. Dis. **8:**987–988.
46. **Orvell, C.** 1976. Identification of paramyxovirus-specific haemolysis-inhibiting antibodies separate from haemagglutinating-inhibiting and neuraminidase-inhibiting antibodies. 2. NDV and mumps virus haemolysis-inhibiting antibodies. Acta Pathol. Microbiol. Scand. B **84**(Suppl. B)**:**451–457.
47. **Pallister, J., D. Middleton, G. Crameri, M. Yamada, R. Klein, T. J. Hancock, A. Foord, B. Shiell, W. Michalski, C. C. Broder, and L. F. Wang.** 2009. Chloroquine administration does not prevent Nipah virus infection and disease in ferrets. J. Virol. **83:**11979–11982.
48. **Parisien, J. P., J. F. Lau, J. J. Rodriguez, C. M. Ulane, and C. A. Horvath.** 2002. Selective STAT protein degradation induced by paramyxoviruses requires both STAT1 and STAT2 but is independent of [alpha]/[beta] interferon signal transduction. J. Virol. **76:**4190–4198.
49. **Park, M. S., A. Garcia-Sastre, J. F. Cros, C. F. Basler, and P. Palese.** 2003. Newcastle disease virus V protein is a determinant of host range restriction. J. Virol. **77:**9522–9532.
50. **Park, M. S., M. L. Shaw, J. Munoz-Jordan, J. F. Cros, T. Nakaya, N. Bouvier, P. Palese, A. Garcia-Sastre, and C. F. Basler.** 2003. Newcastle disease virus (NDV)-based assay demonstrates interferon-antagonist activity for the NDV V protein and the Nipah virus V, W, and C proteins. J. Virol. **77:**1501–1511.
51. **Piguet, V., O. Schwartz, S. Le Gall, and D. Trono.** 1999. The downregulation of CD4 and MHC-I by primate lentiviruses: a paradigm for the modulation of cell surface receptors. Immunol. Rev. **168:**51–63.
52. **Qiao, L., H. Phipps-Yonas, B. Hartmann, T. Moran, S. Sealfon, and F. Hayot.** 2010. Immune response modeling of interferon-β pretreated influenza virus infected human dendritic cells. Biophys. J. **98:**505–514.
53. **Rodriguez, J. J., C. D. Cruz, and C. M. Horvath.** 2004. Identification of the nuclear export signal and STAT-binding domains of the Nipah virus V protein reveals mechanisms underlying interferon evasion. J. Virol. **78:**5358–5367.
54. **Rodriguez, J. J., J.-P. Parisien, and C. M. Horvath.** 2002. Nipah virus V protein evades alpha and gamma interferons by preventing STAT1 and STAT2 activation and nuclear accumulation. J. Virol. **76:**11476–11483.
55. **Sarkkinen, H., O. Ruuskanen, O. Meurman, H. Puhakka, E. Virolainen, and J. Eskola.** 1985. Identification of respiratory virus antigens in middle ear fluids of children with acute otitis media. J. Infect. Dis. **151:**444–448.
56. **Shaw, M. L., W. B. Cardenas, D. Zamarin, P. Palese, and C. F. Basler.** 2005. Nuclear localization of the Nipah virus W protein allows for inhibition of both virus- and Toll-like receptor 3-triggered signaling pathways. J. Virol. **79:**6078–6088.
57. **Shaw, M. L., A. Garcia-Sastre, P. Palese, and C. F. Basler.** 2004. Nipah virus V and W proteins have a common STAT1-binding domain yet inhibit STAT1 activation from the cytoplasmic and nuclear compartments, respectively. J. Virol. **78:**5633–5641.
58. **Tan, C. T.** 2002. Relapsed and late-onset Nipah encephalitis. Ann. Neurol. **51:**703–708.
59. **Ulane, C. M., and C. M. Horvath.** 2002. Paramyxoviruses SV5 and HPIV2 assemble STAT protein ubiquitin ligase complexes from cellular components. Virology **304:**160–166.
60. **Ulane, C. M., J. J. Rodriguez, J.-P. Parisien, and C. M. Horvath.** 2003. STAT3 ubiquitylation and degradation by mumps virus suppress cytokine and oncogene signaling. J. Virol. **77:**6385–6393.
61. **Warren, A. P., D. H. Ducroq, P. J. Lehner, and L. K. Borysiewicz.** 1994. Human cytomegalovirus-infected cells have unstable assembly of major histocompatibility complex class I complexes and are resistant to lysis by cytotoxic T lymphocytes. J. Virol. **68:**2822–2829.
62. **Woods, J. M., K. J. Katschke, Jr., M. Tokuhira, H. Kurata, K. I. Arai, P. L. Campbell, and A. E. Koch.** 2000. Reduction of inflammatory cytokines and prostaglandin E2 by IL-13 gene therapy in rheumatoid arthritis synovium. J. Immunol. **165:**2755–2763.

63. **Yob, J. M.** 2001. Nipah virus infection in bats (order Chiroptera) in peninsular Malaysia. Emerg. Infect. Dis. **7:**439–441.
64. **Yoneyama, M., M. Kikuchi, T. Natsukawa, N. Shinobu, T. Imaizumi, M. Miyagishi, K. Taira, S. Akira, and T. Fujita.** 2004. The RNA helicase RIG-I has an essential function in double-stranded RNA-induced innate antiviral responses. Nat. Immunol. **5:**730–737.
65. **Yu, Z., B. Gotoh, M. Hamaguchi, and Y. Nagai.** 1995. Antiviral action of interferon-beta on Newcastle disease virus: selectivity to the hemagglutinin-neuraminidase gene expression. Med. Microbiol. Immunol. **184:**45–52.
66. **Yuen, T., E. Wurmbach, R. L. Pfeffer, B. J. Ebersole, and S. C. Sealfon.** 2002. Accuracy and calibration of commercial oligonucleotide and custom cDNA microarrays. Nucleic Acids Res. **30:**e48.